

Reaction Rates and Kinetic Isotope Effects of $\text{H}_2 + \text{OH} \rightarrow \text{H}_2\text{O} + \text{H}$ Jan Meisner¹ and Johannes Kästner¹*Institute for Theoretical Chemistry, University of Stuttgart, Pfaffenwaldring 55,
70569 Stuttgart, Germany*

(Dated: 31 May 2016)

We calculated reaction rate constants including atom tunneling of the reaction of dihydrogen with the hydroxy radical down to a temperature of 50 K. Instanton theory and canonical variational theory with microcanonical optimized multidimensional tunneling (CVT/ μ OMT) were applied using a fitted potential energy surface [J. Chem. Phys. 138, 154301 (2013)]. All possible protium/deuterium isotopologues were considered. Atom tunneling increases at about 250 K (200 K for deuterium transfer). Even at 50 K the rate constants of all isotopologues remain in the interval $4 \cdot 10^{-20}$ to $4 \cdot 10^{-17} \text{ cm}^3 \text{ s}^{-1}$, demonstrating that even deuterated versions of the title reaction are possibly relevant to astrochemical processes in molecular clouds. The transferred hydrogen atom dominates the kinetic isotope effect at all temperatures.

I. INTRODUCTION

The reaction of $\text{H}_2 + \text{OH}$ has emerged as a prototype reaction for four-atomic systems. It contributes to fundamental processes in atmospheric chemistry, astrochemistry, and combustion.^{1–3} The reaction being surface catalyzed was shown to be one of the main routes of H_2O formation in the interstellar medium.^{4–7}

On surfaces the reaction was observed at the cryogenic temperature of 10 K through quantum mechanical tunneling of atoms.^{8,9} For the gas phase reaction, a number of studies on this reaction, theoretical^{10–17} as well as experimental^{18–22} down to 200 K has been performed. For an overview of previous experimental and theoretical results, we refer to reviews.^{23,24}

In this article we present reaction rate constants of the title reaction down to 100 K using instanton theory^{25–29} and down to 50 K using CVT/ μ OMT.^{30,31} Instanton theory^{32–41} is a semiclassical theory based on Feynman’s path integrals.⁴² It takes multidimensional tunneling into account while only the optimization of a tunneling path – the instanton – is necessary.⁴³ Instanton theory is meanwhile frequently used to calculate reaction rates in different areas of chemistry.^{39,44–64} Canonical variational theory (CVT) minimizes recrossing compared to transition state theory (TST). It was used with microcanonical optimized multidimensional tunneling (CVT/ μ OMT)^{30,31} was used along with zero curvature tunneling (ZCT),^{65,66} small curvature tunneling (SCT),⁶⁷ large curvature tunneling (LCT),^{68–70} and microcanonical optimized multidimensional tunneling (μ OMT)^{30,31} calculations down to 50 K. ZCT assumes no deviation of the tunneling path from the classical minimum energy path. Compared to that, SCT considers corner-cutting effects and LCT approximates the tunneling path by a linear path from reactants’ valley to products’ valley. The μ OMT method takes into account that the tunneling path depends on the energy by using the maximum of SCT and LCT tunneling probabilities at each energy.^{71,72}

As the four-atomic system of $\text{H}_2 + \text{OH}$ is of fundamental interest, a variety of potential energy surfaces (PES) have been published.^{73–78} Recently, a global potential energy surface fitted by a neural network to UCCSD(T)-F12a/AVTZ data was published (NN1 PES).⁷⁹ This PES was shown to give reliable results in, e.g., the study of the mode specificity of the $\text{H} + \text{HOD}$ reaction.¹⁵ The NN1 PES was therefore applied here as well. Although several studies on thermal rate constants for the title reaction appeared,^{13,17,80} for instance, the semiclassical transition state theory (SCTST) calculations of Nguyen et al.⁸¹ – even

to investigate reaction rate constants of all isotopologues¹³ – it seems that this is the first study which provides rate calculations on the NN1 PES. The reaction profile consisting of the stationary points are shown in Fig. 1.

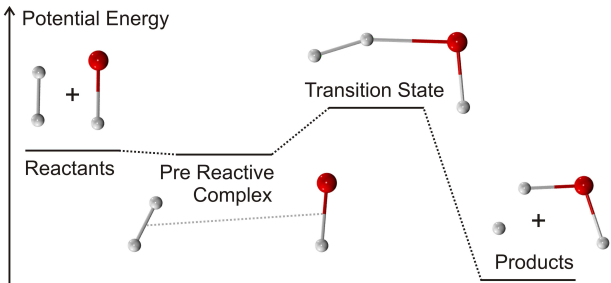


FIG. 1. Potential energy profile of the reaction $\text{H}_2 + \text{OH} \rightarrow \text{H}_2\text{O} + \text{H}$. Relative to the separated reactants, the pre-reactive complex has a potential energy of -2.1 kJ mol^{-1} , the transition state 22.5 kJ mol^{-1} and the separated products $-68.1 \text{ kJ mol}^{-1}$.

For bimolecular reactions, it is in general possible that a (weakly) bound van-der-Waals complex can lead to an increase of the bimolecular reaction rate constant with decreasing temperature. This effect was studied experimentally in the reaction of $\text{HBr} + \text{OH}$ as well as in the reactions with nitric acid or alcohols and OH radicals.⁸²⁻⁸⁴ In these cases, the non-covalent interactions between the two reactants stem from the dipole moments and polarizabilities of the reacting molecules. In contrast to these, H_2 is less polarizable and has no permanent dipole moment. Thus, the intermolecular interaction between H_2 and the OH radical and the impact of the pre-reactive complex (PRC) $[\text{H}_2 \cdots \text{OH}]$ are expected to be small unless the temperature is much lower than considered in this work.

In this study we investigate the temperature dependence of the reaction rate constant and compare it to published values. Furthermore, the temperature dependence for the rate constants for all eight possible isotopologue reactions and the resulting kinetic isotope effects (KIEs) have been studied. At low temperatures (below T_c) tunneling dominates the reaction rate. The nuclear mass has a high impact on the tunneling probability leading to large kinetic isotope effects (KIEs).

II. METHODS

In instanton theory, the instanton, the saddle point corresponding to the transition state, is a closed Feynman path folded back onto itself which spans the barrier region. At high temperature it is short and covers only the top of the barrier while at low temperature it protrudes right into the reactant state region. At the crossover temperature,

$$T_c = \frac{\hbar\omega_{\text{TS}}}{2\pi k_{\text{B}}}, \quad (1)$$

the instanton path generally collapses to a point and the theory becomes inapplicable although extensions above the crossover temperature exist.⁸⁵ Here ω_{TS} is the absolute value of the imaginary frequency at the transition state, \hbar is the reduced Planck’s constant, and k_{B} is Boltzmann’s constant. T_c is mass-dependent: for the title reaction containing protium only it was found to be 276.2 K, while 204.2 K was found for the per-deuterated reaction. In many cases T_c can be used as a cheap and simple indication if atom tunneling is important at the temperature of interest. Following equation (1), whenever ω_{TS} is larger than 1300 cm^{-1} atom tunneling is relevant at room temperature.

The different H/D isotopologues are labeled as $\text{H}^1\text{H}^2\text{OH}^3$ such that the reaction reads $\text{H}^1\text{H}^2 + \text{OH}^3 \rightarrow \text{H}^1 + \text{H}^2\text{OH}^3$. DDOH therefore corresponds to a reaction of OH with D_2 while HDOH corresponds to the reaction $\text{HD} + \text{OH} \rightarrow \text{H} + \text{DOH}$.

Vibrational modes were described by the harmonic approximation of the Feynman path. The translational partition function was in all cases approximated by the one of the ideal gas, which is identical to that of a quantum mechanical particle in a box. The rotational partition function of the transition state was obtained as the geometric mean value of the rotational partition functions of all images along the instanton path treated as rigid quantum rotors. The reactant molecules were, equivalently, treated as rigid rotors. The symmetry number, the order of the rotational subgroup in the molecular point group,⁸⁶ of the individual molecules was taken into account in the rotational partition function, i.e. the one of H_2 and D_2 was divided by two, while the one for HD is not.

The kinetic isotope effects are dominated by tunneling and by the zero-point vibration. Neither the rotational nor the translational contribution have a significant effect on the KIEs.

The NN1 PES⁷⁹ was interfaced with DL-FIND.⁸⁷ Instantons were optimized starting from the classical transition state or by starting from an already optimized instanton of similar

temperature using the adapted Newton–Raphson algorithm implemented in DL-FIND.^{39,40} The convergence criteria for the instanton optimization on the NN1 PES was $5 \cdot 10^{-11}$ atomic units for the maximal component of the gradient. Note, that we use mass-weighted coordinates and gradients with the masses in atomic units, i.e. relative to the electron mass. This influences the convergence criterion.

The instanton is a closed Feynman path with images having pairwise identical coordinates. The full path was represented by 512 images. Convergence with respect to the number of images was tested at the most severe case with the largest distances between adjacent images, the all-H reaction (HHOH) at 100 K. In this case, the rate constant obtained with 4096 images for the full path deviated by only 0.4 % from the value obtained with 512 images and is only 2.4 % higher compared to the value obtained with 194 images. Smaller deviations can be expected at higher temperature or for heavier isotopologues. Thus, we consider the discretization to be converged with respect to the number of images.

To test the quality of the NN1 PES we additionally calculated instanton rate constants with on-the-fly energy calculations at the CCSD(T)-F12 level^{88,89} using the cc-pVDZ-F12 basis set.⁹⁰ The program package Molpro version 2012^{91,92} interfaced to DL-FIND⁸⁷ via ChemShell⁹³ was used for these calculations. Due to the high computational demands of these calculations, 194 images were used and the instanton optimizations were considered converged for all absolute gradient components smaller than 10^{-8} a.u.

Below 100 K, the instanton path for HHOH stretches into the pre-reactive minimum with parts of the path below the energy of the separated reactants, see Fig. 2. Instanton rates are not valid for energies below the separated reactants, so instanton rates are reported only down to 100 K for H-transfer. For the D-transfer the whole instanton path remains above the reactants’ energy for $T > 80$ K. Thus, instanton rates for D-transfer reactions are reported down to 80 K. CVT/ μ OMT was used down to 50 K.

The ZCT, SCT, LCT, and μ OMT calculations on the NN1 PES⁷⁹ have been performed using POLYRATE 2010^{94,95} based on canonical variational transition state theory (CVT).^{71,72} For the LCT calculations, the action integrals (θ integrals) and the sine of the angle between the minimum energy path and the tunneling path were interpolated to 2^{nd} order.

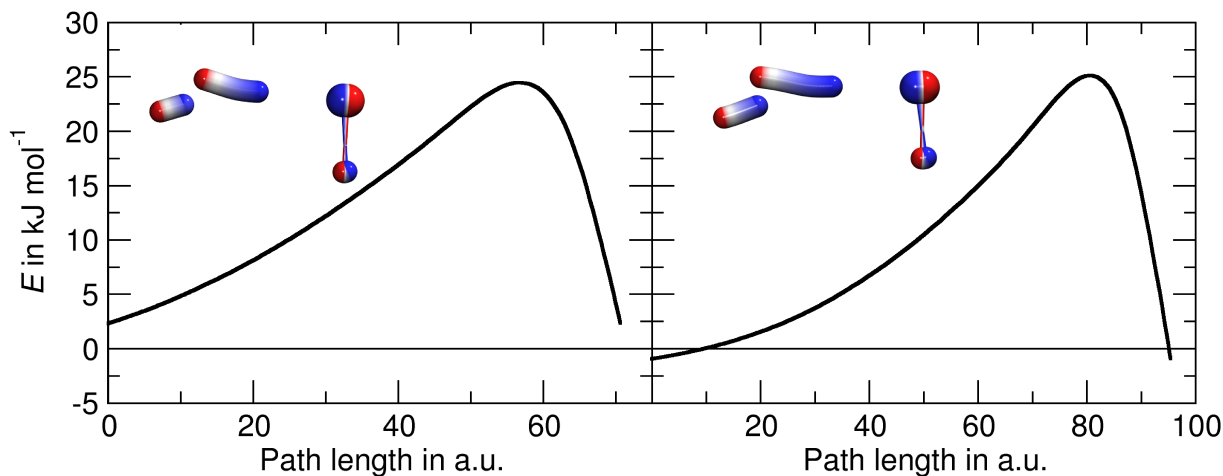


FIG. 2. Potential energy along the instanton path at 130 K (left) and 80 K (right) relative to the energy of the separated reactants. At 130 K the whole instanton path is above the reactant’s energy, at 80 K its ends are below that value. Images of the corresponding instantons are inserted.

III. RESULTS

A. Reaction Rate Constants

The relevant stationary points on the potential energy surface of the title reaction are depicted in Fig. 1. Relative to the separated reactants H_2 and OH , the potential energy on the NN1 PES is $-2.11 \text{ kJ mol}^{-1}$ for the PRC, $22.50 \text{ kJ mol}^{-1}$ for the transition state (TS) and $-68.08 \text{ kJ mol}^{-1}$ for the products ($\text{H} + \text{H}_2\text{O}$). The relative energies of the corresponding stationary points optimized on CCSD(T)-F12/cc-pVDZ-F12 level are -1.77 kJ/mol for the PRC, 23.98 kJ/mol for the TS and -64.94 kJ/mol for the products. The imaginary harmonic frequency is 1206 i cm^{-1} on the NN1 PES and 1199 i cm^{-1} on CCSD(T)-F12/cc-pVDZ-F12 level.

The rate constant of the title reaction has been measured several times using different techniques, see Fig. 3. An Arrhenius plot shows a noticeable curvature already at 300 K and below,^{18,21} which is a clear sign that the reaction is influenced by atom tunneling. Experimental rate constants are available from 1000 K down to 200 K.^{18–22} The different sets agree quite well, typically within 20–30% of the rate constant.

Among the computational studies of this system, Matzkies and Manthe^{17,80} performed

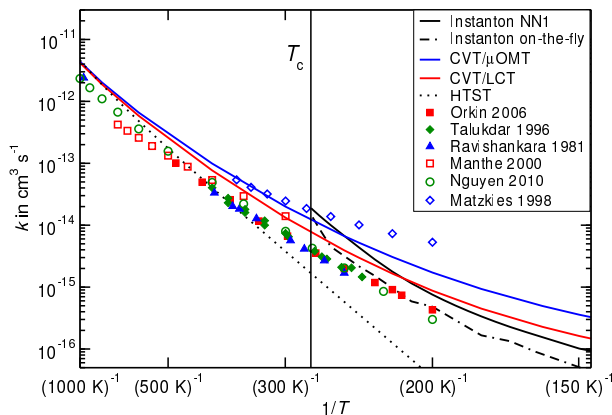


FIG. 3. Reaction rate constants for HHOH compared to literature data. Experimental data: “■” data from²¹, “◆” data from¹⁹, “▲” data from¹⁸; computational data: “□” data from¹⁷, “○” data from⁸¹, “◇” data from⁸⁰.

full-dimensional quantum dynamics calculations on the Schatz–Elgersma PES^{75,76} using the multi-configuration time-dependent Hartree (MCTDH) approach. At $T = 300$ K, the lowest temperature covered by close-coupling calculations employing a rigorously correct statistical sampling scheme for the rotational degrees of freedom,¹⁷ their calculations overestimate the experimental rate constants by about a factor of 2. In an earlier work,⁸⁰ they calculated rate constants down to 200 K, which are more than an order of magnitude higher than the experimental value.²¹ Better agreement with the experimental values was achieved by Nguyen et al.⁸¹ by applying semiclassical transition-state theory (SCTST) on high-level direct-dynamics energies. At 200 K they underestimate the experimental rate constant by a factor of 1.43, which is comparable to the experimental error bar. They furthermore showed that SCT gives significantly higher reaction rate constants at lower temperatures compared to SCTST calculations.⁸¹

For the title reaction containing protium only (HHOH), the crossover temperature is $T_c = 276.2$ K. Using instanton theory, we calculated bimolecular reaction rates using the NN1 PES at $T = 270$ K and below as it is only applicable below T_c . The results are depicted in Fig. 3, numbers are given in the supporting information.⁹⁶ As expected,⁵⁸ instanton theory overestimates the rate constant close to T_c . Agreement is improved at lower temperature. At 220 K our rate constant ($1.78 \cdot 10^{-16} \text{ cm}^3 \text{ s}^{-1}$) is higher by a factor of 1.95 than the results of flash photolysis resonance-fluorescence by Orkin et al.;²¹ at 200 K, the lowest temperature

at which comparison is possible, it is still higher by a factor of 1.76. A higher accuracy of instanton theory can be expected at lower temperature due to the known overestimation close to T_c .⁵⁸

The deviation might reflect a deficiency of the rate theory or the potential. To test the accuracy of the potential, we recalculated instantons and rate constants on-the-fly on CCSD(T)-F12/cc-pVDZ-F12 level without fitting the PES. The reaction rate constants obtained in this way agree better with the experimental result, overestimating it by a factor of 1.49 at 240 K and only by a factor of 1.12 at 200 K. Thus, the NN1 PES leads to a slight overestimation of the rate constants. However, we continue with the NN1 PES as on-the-fly calculations for all isotopologues would be too costly. While the absolute rate constants might be overestimated by a factor of approximately 1.5 to 2.0, one can assume the KIEs incur smaller errors. We assume roughly the same level of accuracy at low temperatures, where no other experimental or computational data are available for comparison.

Given that instanton theory is expected to be more accurate at lower temperatures, the rates using the NN1 PES, which employs a better basis set, are more promising than the direct-dynamics results. Still, the NN1 PES probably shows slight inaccuracies in the region of the configurational space most relevant to tunneling, leading to a slight overestimation of the reaction rate. However, we continue with the NN1 PES. While the absolute rate constants might be overestimated by a factor of approximately 1.5 to 2.0, one can assume the KIEs incur smaller errors. We assume roughly the same level of accuracy at low temperatures, where no other experimental or computational data are available for comparison.

To test the accuracy of the rate theory, we performed CVT/ZCT, SCT, LCT, and μ OMT calculations on the NN1-PES. As in this reaction the SCT rate constant is always higher than the one obtained by LCT, the μ OMT result is virtually indistinguishable from the results obtained by SCT. Therefore no graph for SCT is shown in Fig. 3. At temperatures below 300 K, CVT/LCT (and ZCT) agrees well with instanton theory whereas SCT, and thus μ OMT, give significantly higher rate constants. At 200 K, μ OMT overestimates the reaction rate constants by a factor of 4.0, see table I and Fig. 3.

For comparison, Fig. 3 includes the rate constant calculated by TST with all vibrations treated via quantum partition functions of harmonic oscillators, i.e., accounting for the vibrational zero-point energy but not for tunneling (Harmonic transition state theory, HTST). As expected, it describes the rate constant very well at high temperatures (close to and above

400 K) but deviates significantly below about 300 K.

TABLE I. Reaction rate constants k in $\text{cm}^3 \text{ molecule}^{-1} \text{ s}^{-1}$ at 200 K obtained by different methods. Experimental values are from reference 21.

Exp.	$4.3 \cdot 10^{-16}$
Instanton NN1	$7.56 \cdot 10^{-16}$
Instanton on-the-fly	$4.83 \cdot 10^{-16}$
CVT/ μ OMT	$1.73 \cdot 10^{-15}$
CVT/SCT	$1.73 \cdot 10^{-15}$
CVT/LCT	$8.77 \cdot 10^{-16}$
CVT/ZCT	$7.00 \cdot 10^{-16}$
CVT	$2.76 \cdot 10^{-17}$
HTST	$3.25 \cdot 10^{-17}$

B. Kinetic Isotope Effects

All eight possible isotopologues were investigated. The zero-point energy (ZPE) corrected energies of PRC and TS, as well as T_c are given in table II, the rate constants are shown in Fig. 4. Values of the KIEs at 160 K and 100 K (both instanton and μ OMT), and 50 K (μ OMT) are given in table III.

For reactions with deuterium, the crossover temperature is significantly reduced, see table II. Down to 120 K the curvature of the resulting Arrhenius plot in Fig. 4 is negligible for isotopologues with D-transfer. Defazio et al. already mentioned that tunneling may not be very important in the DDOH case.⁹⁷ This is certainly true in the temperature range where experimental data is available, i.e. above 210 K. At lower temperature the reactions of all isotopologues are dominated by tunneling. A direct comparison between our instanton calculations and experimental data is impossible for any of the deuterated cases, as no data is available below T_c . Above 50 K a clear primary KIE, i.e., depending on the mass of the atom to be transferred, is measurable.

The KIE can stem from differences in zero-point energies or from tunneling.⁹⁸⁻¹⁰⁰ One

TABLE II. ZPE corrected energies of the corresponding characteristic points of the PES in kJ mol^{-1} relative to the separated reactants. The crossover temperature T_c is given in K. E_a refers to the activation energy, the energy difference between TS and PRC.

	PRC	TS	E_a	$E_a(\text{ref}^{13})$	T_c
HHOH	0.54	24.76	24.22	24.41	276.2
HHOD	0.41	23.50	23.09	23.19	276.1
DHOH	0.30	24.13	23.82	23.74	266.0
DHOD	0.17	22.84	22.67	22.48	265.8
HDOH	0.20	25.86	25.66	25.37	208.9
HDOD	0.04	24.57	24.53	24.12	208.8
DDOH	-0.04	25.65	25.69	25.16	204.3
DDOD	-0.22	24.31	24.53	23.86	204.2

may, of course, argue if the harmonic approximation for zero-point energies is good enough to estimate rate constants at such low temperatures. However, our calculated vibrationally adiabatic barriers of the isotopologues agree well (deviation $< 0.7 \text{ kJ mol}^{-1}$) from the literature values obtained by the more elaborate HEAT protocol,¹³ see table II. It was shown previously¹³ that including anharmonicity changes the corresponding barrier height by less than 0.33 kJ mol^{-1} .

Apart from the primary KIE, we observe that deuteration of the hydroxy radical (OD) increases the reaction rate, leading to inverse KIEs. Depending on the deuteration of the other sites, OD increases the rates by factors of 1–3, see table III. The main reason for this effect is that the heavier deuterium atom lowers E_{va} of the transition state by reducing the zero-point energy of the deformation modes of the two molecules with respect to each other.

The reaction rate constants obtained with μOMT are higher than the ones obtained with instanton theory by a factor of 4.2 for HHOH and 5.4 for HDOH at 100 K. It is obvious from Fig. 3 and table I that CVT/ μOMT generally overestimates the reaction rate constants for this reaction, see also Fig. S1, because in μOMT the tunneling path is not optimized. Apart from that, the rate constants seem to follow the same trends, in particular the KIEs obtained by both methods agree reasonably well, see table III.

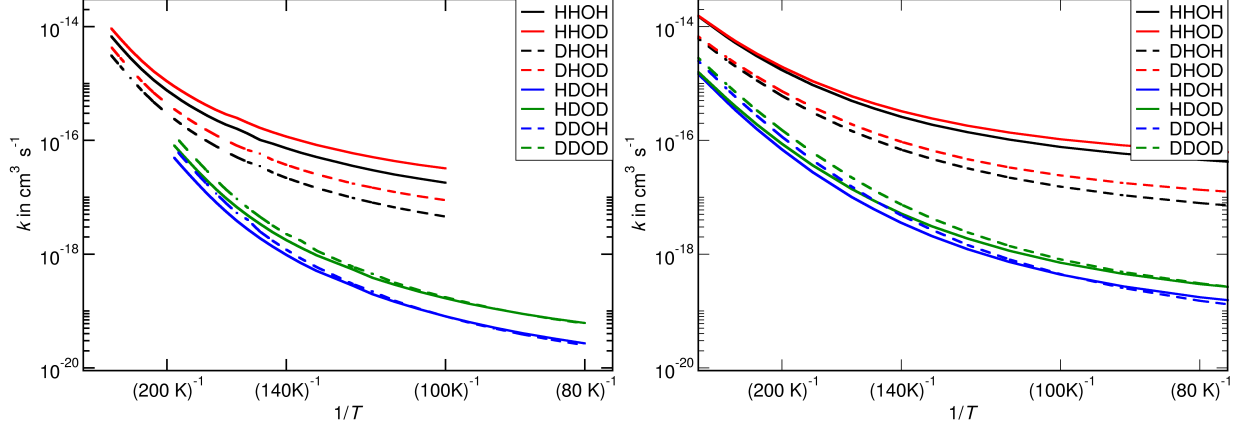


FIG. 4. Temperature dependence of the reaction rate constants of all H/D isotopologues calculated with the instanton method (left) and with CVT/ μ OMT (right).

TABLE III. Kinetic isotope effects at 160 K, 100 K, and 50 K with respect to HHOH.

Isotopes	Instanton		μ OMT		
	160 K	100 K	160 K	100 K	50 K
HHOH	1.00	1.00	1.00	1.00	1.00
DHOH	3.19	3.95	3.37	4.99	6.89
HHOD	0.649	0.561	0.828	0.732	0.610
DHOD	1.99	2.04	2.58	3.19	3.42
HDOH	41.5	224	49.1	176	382
DDOH	30.2	225	32.4	172	558
HDOD	23.9	108	35.4	109	216
DDOD	17.1	104	22.3	95.3	229

Instanton theory provides a dominant tunneling path for each specific temperature. At low temperature, that path is almost temperature-independent. The atoms contribute quite differently to that tunneling path. Geometries and the energy along the instanton path are depicted in Fig. 2. In the low-temperature limit for HHOH, the hydrogen atom to be transferred is delocalized over 1.34 Å, the one that remains as isolated hydrogen atom after the reaction over 0.80 Å. Both oxygen and hydrogen of OH contribute to the tunneling much weaker, they are delocalized over 0.14 and 0.21 Å, respectively. Deuteration changes these

contributions: for HDOH, the transferred deuterium is delocalized over only 1.25 Å while the other tunneling path lengths remain almost unchanged (0.77, 0.15, and 0.21 Å).

We found primary H/D-KIEs of > 200 at 50 K using CVT/ μ OMT. At even lower temperature than reported here, the KIE can be expected to be at least similarly strong. Consequently we expect a significant influence of this reaction and its KIE on the deuterium fractionation of molecules in the interstellar medium.

IV. SUMMARY

We calculated reaction rate constants of $\text{H}_2 + \text{OH} \rightarrow \text{H} + \text{H}_2\text{O}$ down to 100 K using instanton theory and down to 50 K using CVT/ μ OMT on the NN1 PES⁷⁹ for all H/D isotopologues. Atom tunneling sets in at about 250 K for H-transfer and at about 200 K for D-transfer. A significant primary H/D KIE of about 200 is found at 100 K and of 300–600 at 50 K.

At 80–50 K the reaction rate constants of the H-transfer reaction become almost temperature-independent due to atom tunneling. Our results clearly indicate that the title reaction may well be relevant for processes in the interstellar medium at even lower temperature, even including deuterium.

ACKNOWLEDGMENTS

Alexander Denzel is acknowledged for performing the initial calculations. This work was financially supported by the German Research Foundation (DFG) within the Cluster of Excellence in Simulation Technology (EXC 310/2) at the University of Stuttgart.

REFERENCES

- ¹G. Pieterse, M. C. Krol, and T. Röckmann, *Atmos. Chem. Phys.* **9**, 8503 (2009).
- ²T. Rahn, J. M. Eiler, K. A. Boering, P. O. Wennberg, M. C. McCarthy, S. Tyler, S. Schaufliker, S. Donnelly, and E. Atlas, *Nature* **424**, 918 (2003).
- ³S. Gligorovski, R. Strekowski, S. Barbati, and D. Vione, *Chem. Rev.* **115**, 13051 (2015).
- ⁴H. M. Cuppen and E. Herbst, *Astrophys. J.* **668**, 294 (2007).

- ⁵H. M. Cuppen, S. Ioppolo, C. Romanzin, and H. Linnartz, *Phys. Chem. Chem. Phys.* **12**, 12077 (2010).
- ⁶T. Lamberts, H. M. Cuppen, S. Ioppolo, and H. Linnartz, *Phys. Chem. Chem. Phys.* **15**, 8287 (2013).
- ⁷Lamberts, T., Cuppen, H. M., Fedoseev, G., Ioppolo, S., Chuang, K.-J., and Linnartz, H., *Astron. Astrophys.* **570**, A57 (2014).
- ⁸Y. Oba, N. Watanabe, T. Hama, K. Kuwahata, H. Hidaka, and A. Kouchi, *Astrophys. J.* **749**, 67 (2012).
- ⁹J. Meisner and J. Kästner, *Angew. Chem. Int. Ed.*, ASAP, DOI 10.1002/anie.201511028 (2016).
- ¹⁰S. Bhattacharya, A. N. Panda, and H.-D. Meyer, *J. Chem. Phys.* **132**, 214304 (2010).
- ¹¹S. Bhattacharya, A. N. Panda, and H.-D. Meyer, *J. Chem. Phys.* **135**, 194302 (2011).
- ¹²J. Espinosa-Garcia, L. Bonnet, and J. C. Corchado, *Phys. Chem. Chem. Phys.* **12**, 3873 (2010).
- ¹³T. L. Nguyen, J. F. Stanton, and J. R. Barker, *J. Phys. Chem. A* **115**, 5118 (2011).
- ¹⁴B. Fu, E. Kamarchik, and J. M. Bowman, *J. Chem. Phys.* **133**, 164306 (2010).
- ¹⁵B. Fu and D. H. Zhang, *J. Chem. Phys.* **142**, 064314 (2015).
- ¹⁶J. M. Chan, J. A. Bollinger, C. L. Grewell, and D. M. Dooley, *J. Am. Chem. Soc.* **126**, 3030 (2004).
- ¹⁷U. Manthe and F. Matzkies, *J. Chem. Phys.* **113**, 5725 (2000).
- ¹⁸A. R. Ravishankara, J. M. Nicovich, R. L. Thompson, and F. P. Tully, *J. Phys. Chem.* **85**, 2498 (1981).
- ¹⁹R. K. Talukdar, T. Gierczak, L. Goldfarb, Y. Rudich, B. S. M. Rao, and A. R. Ravishankara, *J. Phys. Chem.* **100**, 3037 (1996).
- ²⁰L. N. Krasnoperov and J. V. Michael, *J. Phys. Chem. A* **108**, 5643 (2004).
- ²¹V. L. Orkin, S. N. Kozlov, G. A. Poskrebyshev, and M. J. Kurylo, *J. Phys. Chem. A* **110**, 6978 (2006).
- ²²K.-Y. Lam, D. F. Davidson, and R. K. Hanson, *Int. J. Chem. Kinet.* **45**, 363 (2013).
- ²³J. F. Castillo, *ChemPhysChem* **3**, 320 (2002).
- ²⁴I. W. M. Smith and F. Fleming Crim, *Phys. Chem. Chem. Phys.* **4**, 3543 (2002).
- ²⁵J. S. Langer, *Ann. Phys. (N.Y.)* **41**, 108 (1967).
- ²⁶W. H. Miller, *J. Chem. Phys.* **62**, 1899 (1975).

- ²⁷S. Coleman, Phys. Rev. D **15**, 2929 (1977).
- ²⁸C. G. Callan Jr. and S. Coleman, Phys. Rev. D **16**, 1762 (1977).
- ²⁹E. Gildener and A. Patrascioiu, Phys. Rev. D **16**, 423 (1977).
- ³⁰Y. P. Liu, G. C. Lynch, T. N. Truong, D. Lu, D. G. Truhlar, and B. C. Garrett, J. Am. Chem. Soc. **115**, 2408 (1993).
- ³¹D. G. Truhlar, J. Chem. Soc., Faraday Trans. **90**, 1740 (1994).
- ³²I. Affleck, Phys. Rev. Lett. **46**, 388 (1981).
- ³³S. Coleman, Nucl. Phys. B **298**, 178 (1988).
- ³⁴P. Hänggi, P. Talkner, and M. Borkovec, Rev. Mod. Phys. **62**, 251 (1990).
- ³⁵V. A. Benderskii, D. E. Makarov, and C. A. Wight, Adv. Chem. Phys. **88**, 55 (1994).
- ³⁶M. Messina, G. K. Schenter, and B. C. Garrett, J. Chem. Phys. **103**, 3430 (1995).
- ³⁷J. O. Richardson and S. C. Althorpe, J. Chem. Phys. **131**, 214106 (2009).
- ³⁸S. C. Althorpe, J. Chem. Phys. **134**, 114104 (2011).
- ³⁹J. B. Rommel, T. P. M. Goumans, and J. Kästner, J. Chem. Theory Comput. **7**, 690 (2011).
- ⁴⁰J. B. Rommel and J. Kästner, J. Chem. Phys. **134**, 184107 (2011).
- ⁴¹J. O. Richardson, J. Chem. Phys. **144**, 114106 (2016).
- ⁴²R. P. Feynman, Rev. Mod. Phys. **20**, 367 (1948).
- ⁴³J. Kästner, WIREs Comput. Mol. Sci. **4**, 158 (2014).
- ⁴⁴S. Chapman, B. C. Garrett, and W. H. Miller, J. Chem. Phys. **63**, 2710 (1975).
- ⁴⁵G. Mills and H. Jónsson, Phys. Rev. Lett. **72**, 1124 (1994).
- ⁴⁶G. Mills, H. Jónsson, and G. K. Schenter, Surf. Sci. **324**, 305 (1995).
- ⁴⁷G. Mills, G. K. Schenter, D. E. Makarov, and H. Jónsson, Chem. Phys. Lett. **278**, 91 (1997).
- ⁴⁸W. Siebrand, Z. Smedarchina, M. Z. Zgierski, and A. Fernández-Ramos, Int. Rev. Phys. Chem. **18**, 5 (1999).
- ⁴⁹Z. Smedarchina, W. Siebrand, A. Fernández-Ramos, and Q. Cui, J. Am. Chem. Soc. **125**, 243 (2003).
- ⁵⁰T. Qian, W. Ren, J. Shi, W. E, and P. Shen, Physica A **379**, 491 (2007).
- ⁵¹S. Andersson, G. Nyman, A. Arnaldsson, U. Manthe, and H. Jónsson, J. Phys. Chem. A **113**, 4468 (2009).
- ⁵²T. P. M. Goumans and S. Andersson, Mon. Not. R. Astron. Soc. **406**, 2213 (2010).

- ⁵³T. P. M. Goumans, *Mon. Not. Roy. Astron. Soc.* **415**, 3129 (2011).
- ⁵⁴T. P. M. Goumans, *Mon. Not. Roy. Astron. Soc.* **413**, 26150 (2011).
- ⁵⁵T. P. M. Goumans and J. Kästner, *Angew. Chem., Int. Ed.* **49**, 7350 (2010).
- ⁵⁶H. Jónsson, *Proc. Nat. Acad. Sci. U.S.A.* **108**, 944 (2010).
- ⁵⁷J. Meisner, J. B. Rommel, and J. Kästner, *J. Comput. Chem.* **32**, 3456 (2011).
- ⁵⁸T. P. M. Goumans and J. Kästner, *J. Phys. Chem. A* **115**, 10767 (2011).
- ⁵⁹D. M. Einarsdóttir, A. Arnaldsson, F. Óskarsson, and H. Jónsson, *Lect. Notes Comput. Sci.* **7134**, 45 (2012).
- ⁶⁰J. B. Rommel, Y. Liu, H.-J. Werner, and J. Kästner, *J. Phys. Chem. B* **116**, 13682 (2012).
- ⁶¹M. Kryvohuz and R. A. Marcus, *J. Chem. Phys.* **137**, 134107 (2012).
- ⁶²J. Kästner, *Chem. Eur. J.* **19**, 8207 (2013).
- ⁶³S. Álvarez-Barcia, J. R. Flores, and J. Kästner, *J. Phys. Chem. A* **118**, 78 (2014).
- ⁶⁴M. Kryvohuz, *J. Phys. Chem. A* **118**, 535 (2014).
- ⁶⁵B. C. Garrett, D. G. Truhlar, R. S. Grev, and A. W. Magnuson, *J. Phys. Chem.* **84**, 1730 (1980).
- ⁶⁶D. Truhlar, A. Issacson, R. Skodje, and B. Garrett, *J. Phys. Chem.* **87**, 4554 (1983).
- ⁶⁷R. T. Skodje, D. G. Truhlar, and B. C. Garrett, *J. Phys. Chem.* **85**, 3019 (1981).
- ⁶⁸B. C. Garrett, D. G. Truhlar, A. F. Wagner, and T. H. Dunning Jr., *J. Chem. Phys.* **78**, 4400 (1983).
- ⁶⁹B. C. Garrett, N. Abusalbi, D. J. Kouri, and D. G. Truhlar, *J. Chem. Phys.* **83**, 2252 (1985).
- ⁷⁰A. Fernandez-Ramos and D. G. Truhlar, *J. Chem. Phys.* **114**, 1491 (2001).
- ⁷¹A. Fernández-Ramos, J. A. Miller, S. J. Klippenstein, and D. G. Truhlar, *Chem. Rev.* **106**, 4518 (2006).
- ⁷²A. Fernández-Ramos, B. A. Ellingson, B. C. Garrett, and D. G. Truhlar, “Reviews in computational chemistry,” (Wiley-VCH, Hoboken, NJ, 2007, 2007) Chap. Variational Transition State Theory with Multidimensional Tunneling, pp. 125–232, 1st ed.
- ⁷³G. Ochoa de Aspuru and D. C. Clary, *J. Phys. Chem. A* **102**, 9631 (1998).
- ⁷⁴G.-s. Wu, G. C. Schatz, G. Lendvay, D.-C. Fang, and L. B. Harding, *J. Chem. Phys.* **113**, 3150 (2000).
- ⁷⁵S. P. Walch and T. H. Dunning, *J. Chem. Phys.* **72**, 1303 (1980).

- ⁷⁶G. C. Schatz and H. Elgersma, *Chem. Phys. Lett.* **73**, 21 (1980).
- ⁷⁷M. Yang, D. H. Zhang, M. A. Collins, and S. Lee, *J. Chem. Phys.* **115**, 174 (2001).
- ⁷⁸R. P. A. Bettens, M. A. Collins, M. J. T. Jordan, and D. H. Zhang, *J. Chem. Phys.* **112**, 10162 (2000).
- ⁷⁹J. Chen, X. Xu, X. Xu, and D. H. Zhang, *J. Chem. Phys.* **138**, 154301 (2013).
- ⁸⁰F. Matzkies and U. Manthe, *J. Chem. Phys.* **108**, 4828 (1998).
- ⁸¹T. L. Nguyen, J. F. Stanton, and J. R. Barker, *Chem. Phys. Lett.* **499**, 9 (2010).
- ⁸²J. Ree, Y. H. Kim, and H. K. Shin, *J. Phys. Chem. A* **119**, 3147 (2015).
- ⁸³S. S. Brown, J. B. Burkholder, R. K. Talukdar, and A. R. Ravishankara, *J. Phys. Chem. A* **105**, 1605 (2001).
- ⁸⁴R. J. Shannon, M. A. Blitz, A. Goddard, and D. E. Heard, *Nat. Chem.* **5**, 745 (2013).
- ⁸⁵Y. Zhang, J. B. Rommel, M. T. Cvitaš, and S. C. Althorpe, *Phys. Chem. Chem. Phys.* **16**, 24292 (2014).
- ⁸⁶A. Fernández-Ramos, B. A. Ellingson, R. Meana-Pañeda, J. M. C. Marques, and D. G. Truhlar, *Theor. Chem. Acc.* **118**, 813 (2007).
- ⁸⁷J. Kästner, J. M. Carr, T. W. Keal, W. Thiel, A. Wander, and P. Sherwood, *J. Phys. Chem. A* **113**, 11856 (2009).
- ⁸⁸T. B. Adler, G. Knizia, and H.-J. Werner, *J. Chem. Phys.* **127**, 221106 (2007).
- ⁸⁹T. B. Adler and H.-J. Werner, *J. Chem. Phys.* **130**, 241101 (2009).
- ⁹⁰K. A. Peterson, T. B. Adler, and H.-J. Werner, *J. Chem. Phys.* **128**, 084102 (2008).
- ⁹¹H.-J. Werner, P. J. Knowles, G. Knizia, F. R. Manby, M. Schütz, P. Celani, T. Korona, R. Lindh, A. Mitrushenkov, G. Rauhut, K. R. Shamasundar, T. B. Adler, R. D. Amos, A. Bernhardsson, A. Berning, D. L. Cooper, M. J. O. Deegan, A. J. Dobbyn, F. Eckert, E. Goll, C. Hampel, A. Hesselmann, G. Hetzer, T. Hrenar, G. Jansen, C. Köppl, Y. Liu, A. W. Lloyd, R. A. Mata, A. J. May, S. J. McNicholas, W. Meyer, M. E. Mura, A. Nicklass, D. P. O’Neill, P. Palmieri, D. Peng, K. Pflüger, R. Pitzer, M. Reiher, T. Shiozaki, H. Stoll, A. J. Stone, R. Tarroni, T. Thorsteinsson, and M. Wang, “Molpro, version 2012.1, a package of ab initio programs,” (2012).
- ⁹²H.-J. Werner, P. J. Knowles, G. Knizia, F. R. Manby, and M. Schütz, *WIREs Comput. Mol. Sci.* **2**, 242 (2012).
- ⁹³S. Metz, J. Kästner, A. A. Sokol, T. W. Keal, and P. Sherwood, *WIREs Comput. Mol. Sci.* **4**, 101 (2014).

- ⁹⁴D. Lu, T. N. Truong, V. S. Melissas, G. C. Lynch, Y. Liu, B. C. Garrett, R. Steckler, A. D. Isaacson, S. N. Rai, G. C. Hancock, J. G. Lauderdale, T. Joseph, and D. G. Truhlar, *Comput. Phys. Commun.* **71**, 235 (1992).
- ⁹⁵J. Zheng, S. Zhang, B. Lynch, J. Corchado, Y.-Y. Chuang, P. Fast, W.-P. Hu, Y.-P. Liu, G. Lynch, K. Nguyen, C. Jackels, A. F. Ramos, B. Ellingson, V. Melissas, J. Villà, I. Rossi, E. C. no, J. Pu, T. Albu, R. Steckler, B. Garrett, A. Isaacson, and D. Truhlar, “POLYRATE-version 2010, University of Minnesota, Minneapolis, 2010.” (2010).
- ⁹⁶See supplemental material at [URL will be inserted by AIP] for tables with the values of the reaction rate constants and further comparison of CVT/ μ OMT and instanton reaction rates.
- ⁹⁷P. Defazio and S. K. Gray, *J. Phys. Chem. A* **107**, 7132 (2003).
- ⁹⁸R. Pérez de Tudela, F. J. Aoiz, Y. V. Suleimanov, and D. E. Manolopoulos, *J. Phys. Chem. Lett.* **3**, 493 (2012).
- ⁹⁹Y. V. Suleimanov, R. P. de Tudela, P. G. Jambrina, J. F. Castillo, V. Sáez-Rábanos, D. E. Manolopoulos, and F. J. Aoiz, *Phys. Chem. Chem. Phys.* **15**, 3655 (2013).
- ¹⁰⁰R. Pérez de Tudela, Y. V. Suleimanov, J. O. Richardson, V. S. Rbanos, W. H. Green, and F. J. Aoiz, *J. Phys. Chem. Lett.* **5**, 4219 (2014).

Supplementary Information to: Reaction Rates and Kinetic Isotope Effects of
 $\text{H}_2 + \text{OH} \rightarrow \text{H}_2\text{O} + \text{H}$

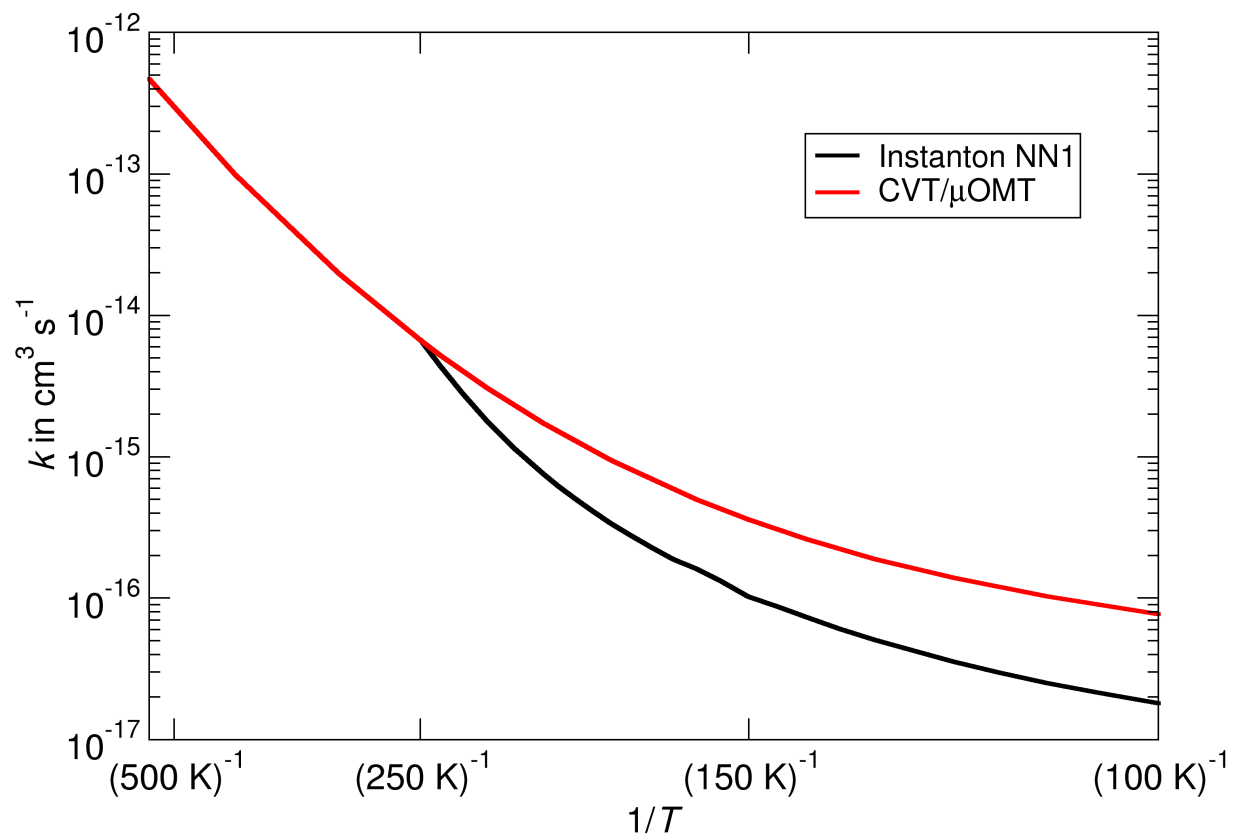


FIG. 5. Comparison of CVT/ μ OMT and instanton reaction rate constants over the whole range of applicability of instanton theory.

TABLE IV. Reaction rate constants for the H-transfer calculated with the instanton method on the NN1 PES. Temperature in K, rate constants in $\text{cm}^3 \text{ molecule}^{-1} \text{ s}^{-1}$.

Temperature	HHOH	DHOH	HHOD	DHOD
100	$1.81 \cdot 10^{-17}$	$4.58 \cdot 10^{-18}$	$3.22 \cdot 10^{-17}$	$8.86 \cdot 10^{-18}$
105	$2.13 \cdot 10^{-17}$	$5.49 \cdot 10^{-18}$	$3.73 \cdot 10^{-17}$	$1.04 \cdot 10^{-17}$
110	$2.51 \cdot 10^{-17}$	$6.61 \cdot 10^{-18}$	$4.34 \cdot 10^{-17}$	$1.23 \cdot 10^{-17}$
115	$2.98 \cdot 10^{-17}$	$8.01 \cdot 10^{-18}$	$5.08 \cdot 10^{-17}$	$1.47 \cdot 10^{-17}$
120	$3.55 \cdot 10^{-17}$	$9.73 \cdot 10^{-18}$	$5.96 \cdot 10^{-17}$	$1.75 \cdot 10^{-17}$
130	$5.06 \cdot 10^{-17}$	$1.45 \cdot 10^{-17}$	$8.30 \cdot 10^{-17}$	$2.53 \cdot 10^{-17}$
135	$6.07 \cdot 10^{-17}$	$1.78 \cdot 10^{-17}$	$9.84 \cdot 10^{-17}$	$3.06 \cdot 10^{-17}$
140	$7.30 \cdot 10^{-17}$	$2.19 \cdot 10^{-17}$	$1.17 \cdot 10^{-16}$	$3.71 \cdot 10^{-17}$
145	$8.77 \cdot 10^{-17}$	$2.73 \cdot 10^{-17}$	$1.39 \cdot 10^{-16}$	$4.55 \cdot 10^{-17}$
150	$1.02 \cdot 10^{-16}$	$3.54 \cdot 10^{-17}$	$1.66 \cdot 10^{-16}$	$5.83 \cdot 10^{-17}$
155	$1.31 \cdot 10^{-16}$	$4.15 \cdot 10^{-17}$	$2.04 \cdot 10^{-16}$	$6.74 \cdot 10^{-17}$
160	$1.61 \cdot 10^{-16}$	$5.06 \cdot 10^{-17}$	$2.49 \cdot 10^{-16}$	$8.12 \cdot 10^{-17}$
165	$1.88 \cdot 10^{-16}$	$6.30 \cdot 10^{-17}$	$2.87 \cdot 10^{-16}$	$9.99 \cdot 10^{-17}$
170	$2.27 \cdot 10^{-16}$	$7.86 \cdot 10^{-17}$	$3.43 \cdot 10^{-16}$	$1.23 \cdot 10^{-16}$
175	$2.76 \cdot 10^{-16}$	$9.80 \cdot 10^{-17}$	$4.14 \cdot 10^{-16}$	$1.52 \cdot 10^{-16}$
180	$3.36 \cdot 10^{-16}$	$1.22 \cdot 10^{-16}$	$5.00 \cdot 10^{-16}$	$1.87 \cdot 10^{-16}$
185	$4.10 \cdot 10^{-16}$	$1.52 \cdot 10^{-16}$	$6.06 \cdot 10^{-16}$	$2.31 \cdot 10^{-16}$
190	$5.02 \cdot 10^{-16}$	$1.90 \cdot 10^{-16}$	$7.36 \cdot 10^{-16}$	$2.86 \cdot 10^{-16}$
195	$6.15 \cdot 10^{-16}$	$2.38 \cdot 10^{-16}$	$8.96 \cdot 10^{-16}$	$3.54 \cdot 10^{-16}$
200	$7.56 \cdot 10^{-16}$	$2.98 \cdot 10^{-16}$	$1.09 \cdot 10^{-15}$	$4.40 \cdot 10^{-16}$
210	$1.15 \cdot 10^{-15}$	$4.73 \cdot 10^{-16}$	$1.64 \cdot 10^{-15}$	$6.88 \cdot 10^{-16}$
220	$1.78 \cdot 10^{-15}$	$7.63 \cdot 10^{-16}$	$2.51 \cdot 10^{-15}$	$1.10 \cdot 10^{-15}$
230	$2.78 \cdot 10^{-15}$	$1.24 \cdot 10^{-15}$	$3.90 \cdot 10^{-15}$	$1.77 \cdot 10^{-15}$
240	$4.37 \cdot 10^{-15}$	$2.00 \cdot 10^{-15}$	$6.07 \cdot 10^{-15}$	$2.82 \cdot 10^{-15}$
250	$6.71 \cdot 10^{-15}$	$3.10 \cdot 10^{-15}$	$9.26 \cdot 10^{-15}$	$4.34 \cdot 10^{-15}$

TABLE V. Reaction rate constants for the D-transfer calculated with the instanton method on the NN1 PES. Temperature in K, rate constants in $\text{cm}^3 \text{ molecule}^{-1} \text{ s}^{-1}$.

T [K]	HDOH	DDOH	HDOD	DDOD
80	$2.70 \cdot 10^{-20}$	$2.50 \cdot 10^{-20}$	$6.14 \cdot 10^{-20}$	$6.02 \cdot 10^{-20}$
84	$3.32 \cdot 10^{-20}$	$3.11 \cdot 10^{-20}$	$7.39 \cdot 10^{-20}$	$7.31 \cdot 10^{-20}$
88	$4.11 \cdot 10^{-20}$	$3.90 \cdot 10^{-20}$	$8.96 \cdot 10^{-20}$	$8.97 \cdot 10^{-20}$
92	$5.11 \cdot 10^{-20}$	$4.93 \cdot 10^{-20}$	$1.10 \cdot 10^{-19}$	$1.11 \cdot 10^{-19}$
96	$6.40 \cdot 10^{-20}$	$6.27 \cdot 10^{-20}$	$1.35 \cdot 10^{-19}$	$1.39 \cdot 10^{-19}$
100	$8.05 \cdot 10^{-20}$	$8.03 \cdot 10^{-20}$	$1.67 \cdot 10^{-19}$	$1.74 \cdot 10^{-19}$
105	$1.08 \cdot 10^{-19}$	$1.10 \cdot 10^{-19}$	$2.19 \cdot 10^{-19}$	$2.33 \cdot 10^{-19}$
110	$1.45 \cdot 10^{-19}$	$1.51 \cdot 10^{-19}$	$2.89 \cdot 10^{-19}$	$3.15 \cdot 10^{-19}$
115	$1.96 \cdot 10^{-19}$	$2.19 \cdot 10^{-19}$	$3.83 \cdot 10^{-19}$	$4.47 \cdot 10^{-19}$
120	$2.80 \cdot 10^{-19}$	$3.00 \cdot 10^{-19}$	$5.41 \cdot 10^{-19}$	$6.01 \cdot 10^{-19}$
130	$5.05 \cdot 10^{-19}$	$5.89 \cdot 10^{-19}$	$9.47 \cdot 10^{-19}$	$1.14 \cdot 10^{-18}$
135	$6.96 \cdot 10^{-19}$	$8.39 \cdot 10^{-19}$	$1.29 \cdot 10^{-18}$	$1.73 \cdot 10^{-18}$
140	$9.69 \cdot 10^{-19}$	$1.20 \cdot 10^{-18}$	$1.77 \cdot 10^{-18}$	$2.25 \cdot 10^{-18}$
145	$1.36 \cdot 10^{-18}$	$1.73 \cdot 10^{-18}$	$2.44 \cdot 10^{-18}$	$3.19 \cdot 10^{-18}$
150	$1.91 \cdot 10^{-18}$	$2.50 \cdot 10^{-18}$	$3.40 \cdot 10^{-18}$	$4.55 \cdot 10^{-18}$
155	$2.72 \cdot 10^{-18}$	$4.00 \cdot 10^{-18}$	$4.77 \cdot 10^{-18}$	$6.53 \cdot 10^{-18}$
160	$3.88 \cdot 10^{-18}$	$5.33 \cdot 10^{-18}$	$6.74 \cdot 10^{-18}$	$9.44 \cdot 10^{-18}$
165	$5.59 \cdot 10^{-18}$	$7.84 \cdot 10^{-18}$	$9.61 \cdot 10^{-18}$	$1.37 \cdot 10^{-17}$
170	$8.08 \cdot 10^{-18}$	$1.16 \cdot 10^{-17}$	$1.38 \cdot 10^{-17}$	$2.01 \cdot 10^{-17}$
175	$1.17 \cdot 10^{-17}$	$1.71 \cdot 10^{-17}$	$1.99 \cdot 10^{-17}$	$2.94 \cdot 10^{-17}$
180	$1.71 \cdot 10^{-17}$	$2.51 \cdot 10^{-17}$	$2.86 \cdot 10^{-17}$	$4.28 \cdot 10^{-17}$
185	$2.46 \cdot 10^{-17}$	$3.64 \cdot 10^{-17}$	$4.10 \cdot 10^{-17}$	$6.16 \cdot 10^{-17}$
190	$3.50 \cdot 10^{-17}$	$5.22 \cdot 10^{-17}$	$5.80 \cdot 10^{-17}$	$8.78 \cdot 10^{-17}$
195	$4.93 \cdot 10^{-17}$	$7.46 \cdot 10^{-17}$	$8.11 \cdot 10^{-17}$	$1.25 \cdot 10^{-16}$

TABLE VI. Reaction rate constants for the HHOH system calculated on-the-fly on CCSD(T)-F12/cc-pVDZ-F12 level with the instanton method. Temperature in K, rate constants in $\text{cm}^3 \text{molecule}^{-1} \text{s}^{-1}$.

T [K]	Rate constants
275	$1.38 \cdot 10^{-14}$
270	$9.38 \cdot 10^{-15}$
260	$4.50 \cdot 10^{-15}$
240	$2.17 \cdot 10^{-15}$
230	$1.52 \cdot 10^{-15}$
220	$9.74 \cdot 10^{-16}$
210	$5.88 \cdot 10^{-16}$
200	$4.83 \cdot 10^{-16}$
180	$1.66 \cdot 10^{-16}$
170	$1.34 \cdot 10^{-16}$
162	$9.00 \cdot 10^{-17}$
145	$3.89 \cdot 10^{-17}$
125	$1.76 \cdot 10^{-17}$
111	$1.09 \cdot 10^{-17}$
100	$7.80 \cdot 10^{-18}$

TABLE VII. Reaction rate constants for the H-transfer calculated with CVT/ μ OMT on the NN1 PES. Temperature in K, rate constants in $\text{cm}^3 \text{ molecule}^{-1} \text{ s}^{-1}$.

T [K]	HHOH	HHOD	DHOH	DHOD
50.00	$2.50 \cdot 10^{-17}$	$4.10 \cdot 10^{-17}$	$3.63 \cdot 10^{-18}$	$7.30 \cdot 10^{-18}$
55.00	$2.69 \cdot 10^{-17}$	$4.32 \cdot 10^{-17}$	$4.02 \cdot 10^{-18}$	$7.85 \cdot 10^{-18}$
60.00	$2.94 \cdot 10^{-17}$	$4.61 \cdot 10^{-17}$	$4.51 \cdot 10^{-18}$	$8.56 \cdot 10^{-18}$
65.00	$3.24 \cdot 10^{-17}$	$4.97 \cdot 10^{-17}$	$5.12 \cdot 10^{-18}$	$9.44 \cdot 10^{-18}$
70.00	$3.60 \cdot 10^{-17}$	$5.42 \cdot 10^{-17}$	$5.87 \cdot 10^{-18}$	$1.05 \cdot 10^{-17}$
75.00	$4.03 \cdot 10^{-17}$	$5.95 \cdot 10^{-17}$	$6.78 \cdot 10^{-18}$	$1.19 \cdot 10^{-17}$
80.00	$4.54 \cdot 10^{-17}$	$6.58 \cdot 10^{-17}$	$7.89 \cdot 10^{-18}$	$1.35 \cdot 10^{-17}$
90.00	$5.85 \cdot 10^{-17}$	$8.23 \cdot 10^{-17}$	$1.09 \cdot 10^{-17}$	$1.78 \cdot 10^{-17}$
100.00	$7.69 \cdot 10^{-17}$	$1.05 \cdot 10^{-16}$	$1.54 \cdot 10^{-17}$	$2.41 \cdot 10^{-17}$
110.00	$1.03 \cdot 10^{-16}$	$1.37 \cdot 10^{-16}$	$2.21 \cdot 10^{-17}$	$3.34 \cdot 10^{-17}$
120.00	$1.39 \cdot 10^{-16}$	$1.81 \cdot 10^{-16}$	$3.21 \cdot 10^{-17}$	$4.68 \cdot 10^{-17}$
130.00	$1.89 \cdot 10^{-16}$	$2.42 \cdot 10^{-16}$	$4.69 \cdot 10^{-17}$	$6.63 \cdot 10^{-17}$
140.00	$2.60 \cdot 10^{-16}$	$3.26 \cdot 10^{-16}$	$6.89 \cdot 10^{-17}$	$9.46 \cdot 10^{-17}$
150.00	$3.59 \cdot 10^{-16}$	$4.42 \cdot 10^{-16}$	$1.01 \cdot 10^{-16}$	$1.35 \cdot 10^{-16}$
160.00	$4.96 \cdot 10^{-16}$	$5.99 \cdot 10^{-16}$	$1.47 \cdot 10^{-16}$	$1.92 \cdot 10^{-16}$
180.00	$9.38 \cdot 10^{-16}$	$1.09 \cdot 10^{-15}$	$3.06 \cdot 10^{-16}$	$3.83 \cdot 10^{-16}$
200.00	$1.73 \cdot 10^{-15}$	$1.95 \cdot 10^{-15}$	$6.05 \cdot 10^{-16}$	$7.33 \cdot 10^{-16}$
220.00	$3.06 \cdot 10^{-15}$	$3.36 \cdot 10^{-15}$	$1.14 \cdot 10^{-15}$	$1.33 \cdot 10^{-15}$
240.00	$5.20 \cdot 10^{-15}$	$5.56 \cdot 10^{-15}$	$2.01 \cdot 10^{-15}$	$2.28 \cdot 10^{-15}$
250.00	$6.68 \cdot 10^{-15}$	$7.06 \cdot 10^{-15}$	$2.61 \cdot 10^{-15}$	$2.94 \cdot 10^{-15}$
298.00	$1.92 \cdot 10^{-14}$	$1.94 \cdot 10^{-14}$	$7.94 \cdot 10^{-15}$	$8.45 \cdot 10^{-15}$
300.00	$2.00 \cdot 10^{-14}$	$2.01 \cdot 10^{-14}$	$8.20 \cdot 10^{-15}$	$8.79 \cdot 10^{-15}$
400.00	$9.87 \cdot 10^{-14}$	$9.33 \cdot 10^{-14}$	$4.17 \cdot 10^{-14}$	$4.17 \cdot 10^{-14}$
600.00	$6.30 \cdot 10^{-13}$	$5.86 \cdot 10^{-13}$	$2.76 \cdot 10^{-13}$	$2.60 \cdot 10^{-13}$
800.00	$2.02 \cdot 10^{-12}$	$1.76 \cdot 10^{-12}$	$8.48 \cdot 10^{-13}$	$7.77 \cdot 10^{-13}$
1000.00	$4.35 \cdot 10^{-12}$	$3.76 \cdot 10^{-12}$	$1.86 \cdot 10^{-12}$	$1.67 \cdot 10^{-12}$
1250.00	$8.96 \cdot 10^{-12}$	$7.61 \cdot 10^{-12}$	$3.90 \cdot 10^{-12}$	$3.49 \cdot 10^{-12}$
1500.00	$1.56 \cdot 10^{-11}$	$1.32 \cdot 10^{-11}$	$6.92 \cdot 10^{-12}$	$6.20 \cdot 10^{-12}$
2000.00	$3.63 \cdot 10^{-11}$	$3.06 \cdot 10^{-11}$	$1.64 \cdot 10^{-11}$	$1.47 \cdot 10^{-11}$

TABLE VIII. Reaction rate constants for the D-transfer calculated with CVT/ μ OMT on the NN1 PES. Temperature in K, rate constants in $\text{cm}^3 \text{ molecule}^{-1} \text{ s}^{-1}$.

T [K]	HDOH	HDOD	DDOH	DDOD
50.00	$6.54 \cdot 10^{-20}$	$1.16 \cdot 10^{-19}$	$4.48 \cdot 10^{-20}$	$1.09 \cdot 10^{-19}$
55.00	$7.42 \cdot 10^{-20}$	$1.30 \cdot 10^{-19}$	$5.25 \cdot 10^{-20}$	$1.23 \cdot 10^{-19}$
60.00	$8.55 \cdot 10^{-20}$	$1.49 \cdot 10^{-19}$	$6.28 \cdot 10^{-20}$	$1.43 \cdot 10^{-19}$
65.00	$1.00 \cdot 10^{-19}$	$1.74 \cdot 10^{-19}$	$7.65 \cdot 10^{-20}$	$1.69 \cdot 10^{-19}$
70.00	$1.19 \cdot 10^{-19}$	$2.05 \cdot 10^{-19}$	$9.49 \cdot 10^{-20}$	$2.02 \cdot 10^{-19}$
75.00	$1.43 \cdot 10^{-19}$	$2.46 \cdot 10^{-19}$	$1.19 \cdot 10^{-19}$	$2.47 \cdot 10^{-19}$
80.00	$1.75 \cdot 10^{-19}$	$2.98 \cdot 10^{-19}$	$1.52 \cdot 10^{-19}$	$3.06 \cdot 10^{-19}$
90.00	$2.72 \cdot 10^{-19}$	$4.52 \cdot 10^{-19}$	$2.56 \cdot 10^{-19}$	$4.87 \cdot 10^{-19}$
100.00	$4.38 \cdot 10^{-19}$	$7.08 \cdot 10^{-19}$	$4.46 \cdot 10^{-19}$	$8.07 \cdot 10^{-19}$
110.00	$7.25 \cdot 10^{-19}$	$1.14 \cdot 10^{-18}$	$7.99 \cdot 10^{-19}$	$1.38 \cdot 10^{-18}$
120.00	$1.22 \cdot 10^{-18}$	$1.87 \cdot 10^{-18}$	$1.45 \cdot 10^{-18}$	$2.41 \cdot 10^{-18}$
130.00	$2.08 \cdot 10^{-18}$	$3.09 \cdot 10^{-18}$	$2.66 \cdot 10^{-18}$	$4.24 \cdot 10^{-18}$
140.00	$3.55 \cdot 10^{-18}$	$5.14 \cdot 10^{-18}$	$4.83 \cdot 10^{-18}$	$7.44 \cdot 10^{-18}$
150.00	$6.03 \cdot 10^{-18}$	$8.52 \cdot 10^{-18}$	$8.68 \cdot 10^{-18}$	$1.30 \cdot 10^{-17}$
160.00	$1.01 \cdot 10^{-17}$	$1.40 \cdot 10^{-17}$	$1.53 \cdot 10^{-17}$	$2.22 \cdot 10^{-17}$
180.00	$2.75 \cdot 10^{-17}$	$3.61 \cdot 10^{-17}$	$4.44 \cdot 10^{-17}$	$6.08 \cdot 10^{-17}$
200.00	$6.93 \cdot 10^{-17}$	$8.69 \cdot 10^{-17}$	$1.16 \cdot 10^{-16}$	$1.52 \cdot 10^{-16}$
220.00	$1.60 \cdot 10^{-16}$	$1.92 \cdot 10^{-16}$	$2.72 \cdot 10^{-16}$	$3.41 \cdot 10^{-16}$
240.00	$3.40 \cdot 10^{-16}$	$3.94 \cdot 10^{-16}$	$5.81 \cdot 10^{-16}$	$7.05 \cdot 10^{-16}$
250.00	$4.82 \cdot 10^{-16}$	$5.49 \cdot 10^{-16}$	$8.24 \cdot 10^{-16}$	$9.85 \cdot 10^{-16}$
298.00	$2.02 \cdot 10^{-15}$	$2.14 \cdot 10^{-15}$	$3.41 \cdot 10^{-15}$	$3.81 \cdot 10^{-15}$
300.00	$2.13 \cdot 10^{-15}$	$2.25 \cdot 10^{-15}$	$3.60 \cdot 10^{-15}$	$4.01 \cdot 10^{-15}$
400.00	$1.68 \cdot 10^{-14}$	$1.63 \cdot 10^{-14}$	$2.72 \cdot 10^{-14}$	$2.74 \cdot 10^{-14}$
600.00	$1.72 \cdot 10^{-13}$	$1.55 \cdot 10^{-13}$	$2.70 \cdot 10^{-13}$	$2.57 \cdot 10^{-13}$
800.00	$6.42 \cdot 10^{-13}$	$5.59 \cdot 10^{-13}$	$1.01 \cdot 10^{-12}$	$9.36 \cdot 10^{-13}$
1000.00	$1.56 \cdot 10^{-12}$	$1.34 \cdot 10^{-12}$	$2.50 \cdot 10^{-12}$	$2.28 \cdot 10^{-12}$
1250.00	$3.50 \cdot 10^{-12}$	$2.98 \cdot 10^{-12}$	$5.71 \cdot 10^{-12}$	$5.16 \cdot 10^{-12}$
1500.00	$6.45 \cdot 10^{-12}$	$5.44 \cdot 10^{-12}$	$1.08 \cdot 10^{-11}$	$9.61 \cdot 10^{-12}$
2000.00	$1.60 \cdot 10^{-11}$	$1.34 \cdot 10^{-11}$	$2.71 \cdot 10^{-11}$	$2.40 \cdot 10^{-11}$